STUDY OF THE PRODUCTION OF Z BOSON PAIRS IN e^+e^- COLLISIONS AT LEP WITH THE L3 DETECTOR

Simonetta Gentile
CERN, Universitá "La Sapienza" Roma

Abstract

At the center-of-mass energy of 189 GeV attained by the LEP e^+e^- collider in 1998, the production of Z pairs is enhanced with respect to the threshold at 183 GeV. The higher cross section and the high integrated luminosity of the 1998 run give a statistical significant ZZ sample. We report on the study of all visible decay modes of a Z pair. The cross section is measured to be in agreement with the Standard Model predictions. No evidence for the existence of anomalous triple gauge boson ZZZ and ZZγ couplings is found and limits on their values are set.

1 Introduction

The production of on-shell Z boson pairs has become accessible at LEP in 1997 and 1998 with the center-of-mass energy at and above the ZZ threshold ($\sqrt{s}$=183 GeV,$\sqrt{s}$=189 GeV). The results discussed are main based on to an integrated luminosities are 176.4 pb^{-1} and 55.3 pb^{-1} at these energies. In this note we present the L3 measurement of the Z pair production and the interpretation with anomalous ZZZ and ZZγ coupling in all the visible decay modes, namely, $\ell^+\ell^-\mathrm{q\bar{q}}$, $\ell^+\ell^-\ell'^+\ell'^-$, $\ell^+\ell^-\nu\bar{\nu}$, $\mathrm{q\bar{q}}\nu\bar{\nu}$ and $\mathrm{q\bar{q}q'\bar{q}'}$ [1, 2].

The interest of this process at LEP is for twofold. Firstly, the study of ZZ events carries new experimental information about the structure of electroweak interactions, thus allowing new tests of Standard Model (SM) predictions in $\mathrm{e^+e^-}$ collissions at energy never attained before. Secondly, measurements of their production rate is extremely important for Higgs search, in HZ associated production, when the Higgs mass is close to the Z mass because Z pairs constitue an irreducible background.

2 Physics Process and ZZ signal

In the Standard Model the process $\mathrm{e^+e^-} \rightarrow$ ZZ is described by the conversion diagram in via the t-channel exchange of an electron. (Fig.1)

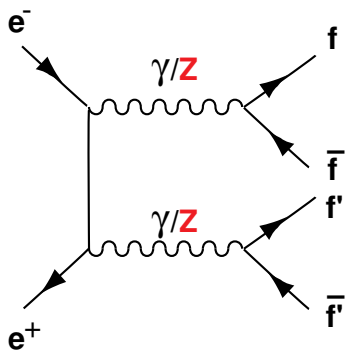

Figure 1: *ZZ conversion diagram.*

However others diagram are contributing to the same four fermions final state as: non-resonant (Fig.2) or involving WW (Fig.3).

The EXCALIBUR [3] Monte Carlo is used to simulate the neutral-current four-fermion events. The on-shell ZZ signal is defined by phase-space cuts at generator level. The masses of the generated fermion pairs in the final state are required to be in the range between 70 GeV and 105 GeV. If the four fermions are of the same

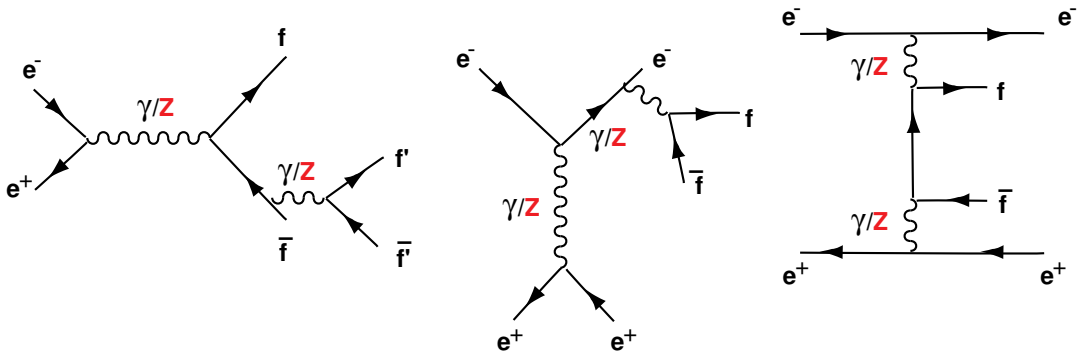

Figure 2: *non-resonant diagram.*

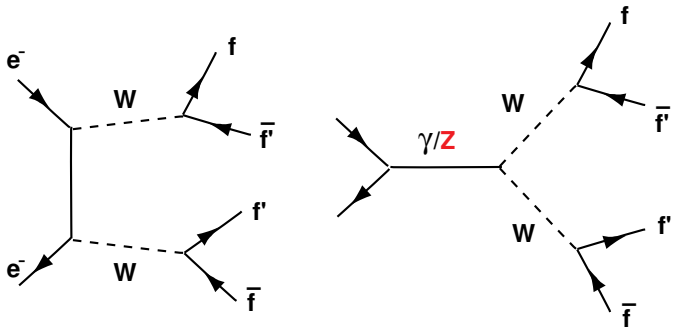

Figure 3: *non-resonant diagram.*

flavor, for at least one of the two possible fermion pair combinations, the fermion pair masses must be in the range mentioned above. There is a large contribution from W exchange in the final states $u\bar{u}d\bar{d}$, $c\bar{c}s\bar{s}$ and $\nu_\ell\bar{\nu}_\ell\ell^+\ell^-$ ($\ell = e, \mu, \tau$). To reduce this contribution we require that the masses of the fermion pairs susceptible to come from a W decay be either smaller than 75 GeV or larger than 85.

The total expected ZZ cross section within these cuts is 0.25 pb at 183 GeV, and 0.62 pb at 189 GeV,(Fig.4). In Tab. 1, the contributions from different final states are reported.

3 On-shell ZZ selection

Different selections for *llqq*, *llll*, *llnn*, *llqq*, *qqqq* channels are optimized for events with high invariant mass of fermion pairs, based on their topology and taking into account the possible sources of background.

Table 1: *Cross section and Decay Branching Fraction for ZZ signal.*

	σ(pb)	B.R.
$q\bar{q}q'\bar{q}'$	0.290	46.8%
$q\bar{q}\nu\bar{\nu}$	0.170	27.4%
$\ell^+\ell^- q\bar{q}$	0.097	15.6%
$\ell^+\ell^-\nu\bar{\nu}$	0.027	4.4%
$\ell^+\ell^-\ell'^+\ell'^-$	0.011	1.8%
$\nu\bar{\nu}\nu'\bar{\nu}'$	0.025	4.0%
Total	0.620	100%

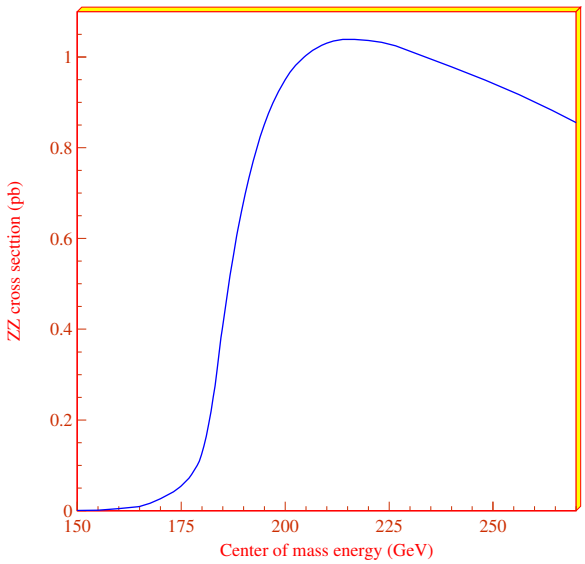

Figure 4: *EXCALIBUR predicted cross section.*

3.1 The ZZ $\rightarrow \ell^+\ell^- q\bar{q}$ channel

The ZZ$\rightarrow$ $\ell^+\ell^- q\bar{q}$ selections are performed for final states with electrons, muons and taus. These events are characterized by an hadronic and a leptonic part. The thresholds are applied on the visible energy and lepton energy. The opening angle between the two electrons or muons and the two jets has to exceed 120°. The $e^+e^- q\bar{q}$ and $\mu^+\mu^- q\bar{q}$ events are subject to the DURHAM algorithm requiring $\log(Y_{34}) \geq -6$, with Y_{34} the parameter separating an event from a four-jet to a three-jet topology. For the $e^+e^- q\bar{q}$ channel we require in addition the invariant mass of the two electrons to be larger than 70 GeV and the ratio of the missing transverse momentum to the visible energy to be less than 0.1.
The $\tau^+\tau^- q\bar{q}$ events are selected by a tau identification and a jet based algorithms. The τ can decay into isolated electrons or muons, or as an isolated low-multiplicity

jet with 1 or 3 tracks and unit charge. The opening angle between the two τ candidates and between the two jets must be larger than 130°. Their invariant masses must be within 70 GeV and 120 GeV.

The efficiencies of $\ell^+\ell^-\mathrm{q\bar{q}}$ selections are different according to the lepton flavour: at 189 GeV are 79% for $\mathrm{e^+e^-q\bar{q}}$,61% for $\mu + \mu^-\mathrm{q\bar{q}}$ and 36% for $\tau^+\tau^-\mathrm{q\bar{q}}$. The results for the $\ell^+\ell^-\mathrm{q\bar{q}}$ event selections at 189 GeV are summarized in Tab. 2.

The spectra of the mass obtained from a kinematic fit, imposing four-momentum conservation and equal masses of the lepton and the jet pair, are shown in Fig. 5 for data and Monte Carlo samples. The background is dominated by $\mathrm{W^+W^-} \to \ell\nu\mathrm{q\bar{q}}$ events. The remaining background consists of $\mathrm{e^+e^-} \to \mathrm{q\bar{q}}(\gamma)$. The errors on signal and background predictions are dominated by uncertainties in the energy scale, the lepton identification and isolation. An error of 15% on the expected number of background events and 4% on the signal efficiency are assigned.

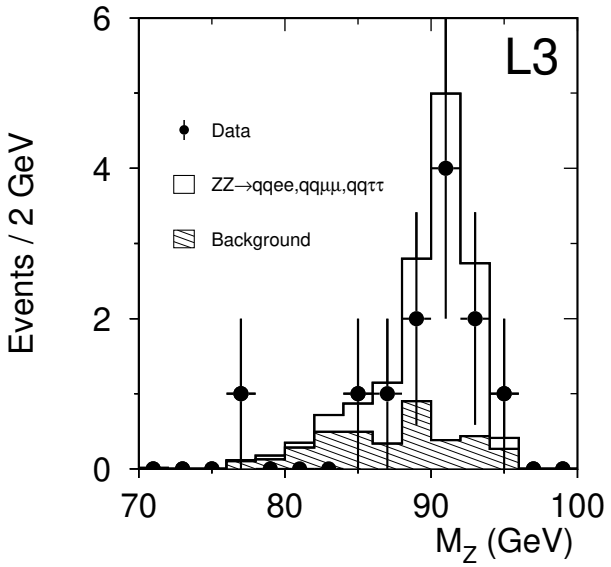

Figure 5: *Mass distribution of selected* $\mathrm{ZZ} \to \ell^+\ell^-\mathrm{q\bar{q}}$ *at 189 GeV.*

3.2 The $\mathrm{ZZ} \to \ell^+\ell^-\ell'^+\ell'^-$, $\ell^+\ell^-\nu\bar{\nu}$ channels

The $\mathrm{ZZ} \to \ell^+\ell^-\ell'^+\ell'^-$ selection is developed for all charged leptonic final states (except events with four τ in the final state). At least four leptons are required in the event. The lepton energy requested is 3 GeV, increased to 15 GeV for electrons. The

Table 2: *Preliminary results of signal efficiencies, expected number of signal and background events and data at 189 GeV.* [a]($e^+e^-\nu\bar{\nu}$),[b] ($\mu^+\mu^-\nu\bar{\nu}$),[c] ($e^+e^-q\bar{q}$),[d] ($\mu^+\mu^-q\bar{q}$),[e] ($\tau^+\tau^-q\bar{q}$)

Process ZZ →	Signal efficiency (%)	Signal events	Background events	Data events
$\ell^+\ell^-q\bar{q}$	$73^c, 55^d, 28^e$	10	5	14
$\ell^+\ell^-\ell'^+\ell'^-$	28-66	0.7	0.6	2
$\ell^+\ell^-\nu\bar{\nu}$	$29^a, 21^b$	0.7	1.2	3
$q\bar{q}\nu\bar{\nu}$	61	19	39	61
$q\bar{q}q'\bar{q}'$	58	32	663	714

invariant masses of the combinations of two same flavor leptons are then calculated and the lepton pair whose mass is the closest to the Z boson mass is chosen. This mass and the recoil mass to the chosen lepton pair are required to be in the range between 70 GeV and 105 GeV.

The $\ell^+\ell^-\nu\bar{\nu}$ events are selected requiring two electrons or two muons. The visible energy is required in the range between 80 GeV and 100 GeV, and the event should be characterized by low multiplicity: less than 3 tracks and less than 6 energy deposits in the calorimeters. The lepton pair mass must be in the range 70 GeV to 105 GeV and the mass recoiling against the leptons in the range 70 GeV to 100 GeV.

The main background to these channels are constituted by lepton pair production as well as neutral and charged-current four-fermion events outside the ZZ signal definition cuts. The errors on the expected signal and background events are due to the lepton identification and the finite Monte Carlo statistics. The signal efficiency, which dependsthe final state, the expected signal and background and the observed events at 189 GeV are reported in Tab.2. Systematic errors of 25% and 10% are assigned to the expected number of background and signal events, respectively, for $\ell^+\ell^-\ell'^+\ell'^-$, and 10% for both signal and background for the $\ell^+\ell^-\nu\bar{\nu}$ final state.

3.3 The ZZ →$q\bar{q}\nu\bar{\nu}$ channel

The selection of ZZ→ $q\bar{q}\nu\bar{\nu}$ events is based on their high multiplicity and missing energy. An energy deposition in the electromagnetic calorimeter larger than 10 GeV is required. The invariant mass of the two jets, M_{vis}, must be in the range 60 GeV to 125 GeV. The contribution of non resonnant diagram is suppressed by requiring the energy in the low polar angle calorimeters to be smaller than 10 GeV. The

$e^+e^- \rightarrow q\bar{q}(\gamma)$ events are rejected requiring the transverse missing energy larger than 5 GeV and the longitudinal momentum less than 50% of the visible energy. To distinguish the signal from W^+W^- background, the discriminant variable NN is constructed using a neural network approach. The inputs to the neural network include event shape variables, the event mass, the masses of the two jets and the total missing momentum.

The visible mass distribution, M_{vis}, is shown in Fig.6 for the 189 GeV data and the corresponding signal efficiency, the expected signal and background and the observed events are reported in Table 2. The errors on signal and background expectations are mainly determined by the uncertainty on the energy calibration and the finite Monte Carlo statistics: they are 4% and 5% for signal and background, respectively.

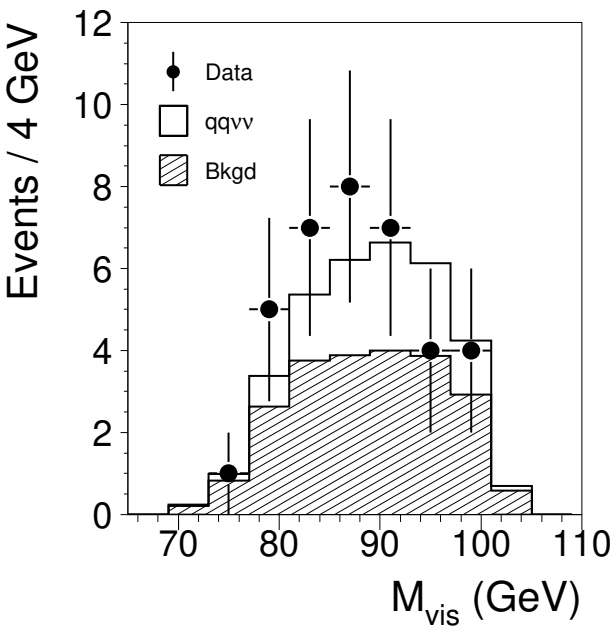

Figure 6: *Mass distribution of selected* $ZZ \rightarrow q\bar{q}\nu\bar{\nu}$ *at 189 GeV.*

3.4 The $ZZ \rightarrow q\bar{q}q'\bar{q}'$ channel

The $ZZ \rightarrow q\bar{q}q'\bar{q}'$ event selection is based on the high multilplicity characteristics of the hadronic event and on the visible energy close to center-of-mass energy. Each of the four jets in the event is required to have more than 4 tracks to suppress the

contamination of τ in the final state. Of the three possible pairing combinations, the one with minimum mass χ^2 to the assumption of a Z pair is chosen.

A neural network method is used to distinguish these events from the $e^+e^- \to q\bar{q}(\gamma)$ and $e^+e^- \to W^+W^-$ backgrounds. The input variables are chosen for the event topological variables, kinematic variables of jets, ratio of energies and opening angles of the jets, and the χ^2 values of equal mass fits for W^+W^- or ZZ pairs hypotheses. The discriminant variable, $\xi = \mathrm{NN_{ZZ}}(1-\mathrm{NN_{qq}})(1-\mathrm{NN_{WW}})(2\mathrm{M_{5C}}/\sqrt{s})$, is a convolution of the three neural network outputs for $e^+e^- \to q\bar{q}(\gamma)$, W^+W^- and ZZ hypotesis, denoted as $\mathrm{NN_{qq}}$, $\mathrm{NN_{WW}}$ and $\mathrm{NN_{ZZ}}$, respectively, and the invariant mass, $\mathrm{M_{5C}}$, is obtained from a kinematic fit imposing four-momentum conservation and equal mass for the two di-jets. The distributions of the discriminant varaiable is shown in Fig. 7. The signal efficiency, expected signal, background and observed data events are reported in Tab. 2 for the 189 GeV data. The errors on signal and background expectations are mainly determined by the uncertainty on the energy calibration and the finite Monte Carlo statistics: they are 6% and 4% for signal and background, respectively.

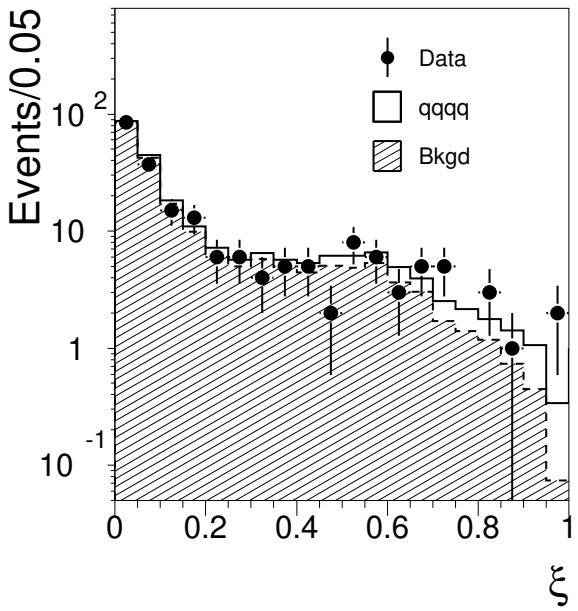

Figure 7: *Discriminant variable of selected* $\mathrm{ZZ} \to q\bar{q}q'\bar{q}'$ *at 189 GeV.*

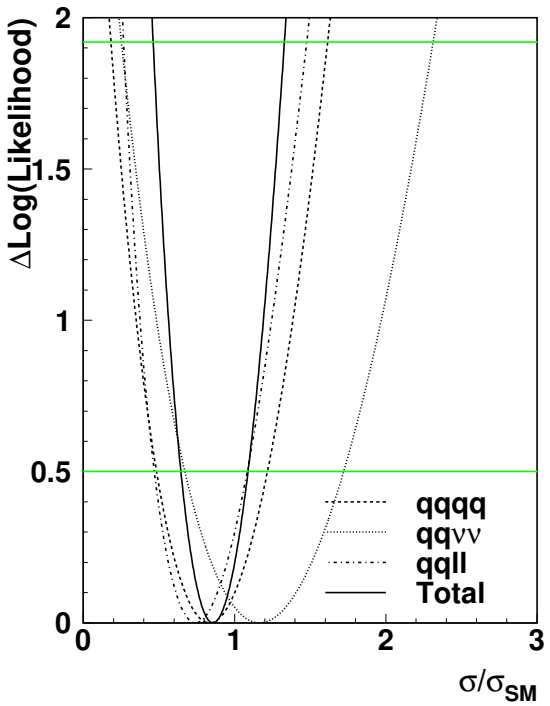

Figure 8: *The likelihoods as a function of the ratio of measured and Standard Model predicted cross-section at 189 GeV. The higher line corresponds to 95% of probability, the lower to 68%*

4 Measurement of the ZZ cross section

The spectra of all decay channels are used in a binned Poissonian log-likelihood fit for the ratio of the measured cross section to the Standard Model value as predicted by EXCALIBUR, $x = \sigma_{ZZ}/\sigma_{ZZ}^{SM}$. The likelihoods of the most significant channels are combined as:

$$Ł(x|N_{ij}, b_{ij}, s_{ij}) = -\log \Pi_{\rm ch}^{i} \Pi_{\rm bins}^{j} \frac{e^{-(xs_{ij}+b_{ij})} \cdot (xs_{ij}+b_{ij})^{N_{ij}}}{N_{ij}!} \qquad (1)$$

where the index i runs over $\ell^+\ell^-\ell'^+\ell'^-, \ell^+\ell^-\mathrm{q\bar{q}}, \ell^+\ell^-\nu\bar{\nu}, \mathrm{q\bar{q}q'\bar{q}'}$ analysis and j over number of bins that each of them has for the most discriminating variable to use in the fit, as for example those of Fig.5,6,7. In the above formula s_{ij},b_{ij} and N_{ij} are, respectively, the Standard Model signal and background expectations and the data contents in the j-th bin for the i-th analysis. The likelihoods are shown in Fig. 8. The measured cross sections are

$$\sigma_{\rm ZZ} = 0.30^{+0.22\ +0.07}_{-0.16\ -0.03} \ \text{pb} \quad (\sigma_{\rm ZZ}^{\rm SM} = 0.25\ \text{pb}), \quad \text{at 183 GeV;}$$
$$\sigma_{\rm ZZ} = 0.54^{+0.16}_{-0.14} \ \text{pb} \quad (\sigma_{\rm ZZ}^{\rm SM} = 0.62\ \text{pb}), \quad \text{at 189 GeV, preliminary.}$$

At 183 GeV, the systematic error is estimated taking into account the errors on signal and background expectations reported in Tab. 2. The error at 189 GeV is statistical only. The measured cross section values are in good agreement with the Standard Model, as shown in Fig. 9

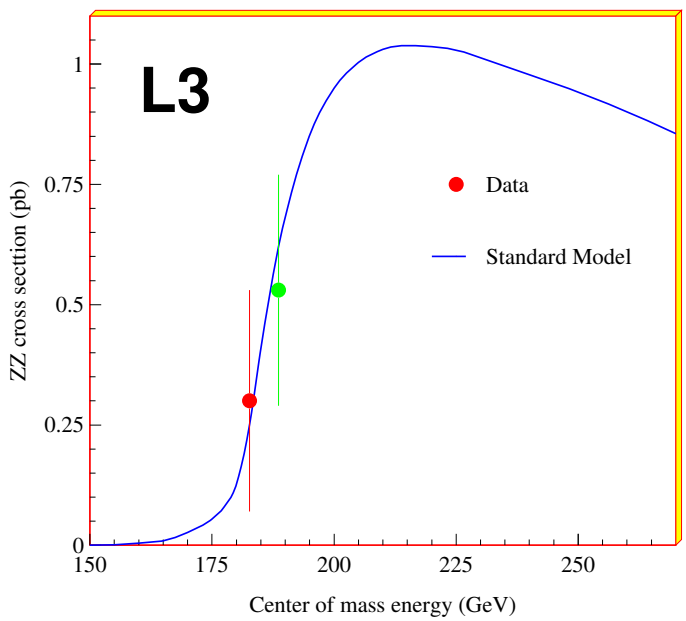

Figure 9: *EXCALIBUR predicted cross section with the experimental measurements.*

5 Limits on anomalous coupling

Possible deviations from the Standard Model predictions in ZZ production can be described using the most general Lorentz invariant expressions, as given in Ref. [4]. They are interpreted in term of anomalous ZZγ and ZZZ couplings. The diagrams contributing at first order to the process $e^+e^- \to ZZ$ have been discussed in Sec.1 and anomalous coupling arises from interactions of type shown in Fig. 10. In this framework, the deviations from Standard Model are described by means of four anomalous couplings f_i^V $(i = 4, 5; V = \gamma, Z)$, where the V superscript corresponds to an anomalous coupling ZZV. The anomalous couplings f_5^V lead to violation of C and P symmetries while f_4^V introduces CP violation. At tree level these couplings are zero in the Standard Model. All anomalous contributions increase with the center-of-mass-energy in the collision. Their effects manifest in three ways: as change in the observed total cross section $e^+e^- \to ZZ$, as a change in the average polarization of Z bosons and a modification of the angular distribution of the Z.

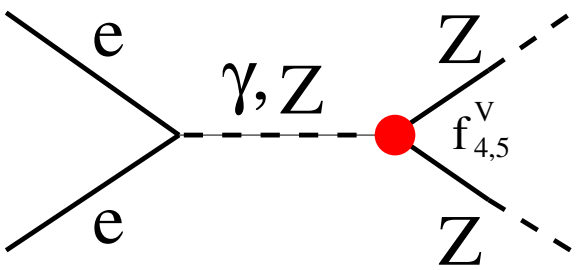

Figure 10: *Diagram with anomalous $ZZ\gamma$ and ZZZ couplings to the process* $e^+e^- \to ZZ$

Table 3: *Coupling Parameters at different center-of-mass energies.*

183 GeV	$-3.6 \leq f_4^Z \leq 3.4$	$-8.4 \leq f_5^Z \leq 7.9$	$-2.1 \leq f_4^\gamma \leq 2.1$	$-4.9 \leq f_5^\gamma \leq 4.8$
189 GeV	$-1.8 \leq f_4^Z \leq 1.8$	$-5.5 \leq f_5^Z \leq 5.4$	$-1.1 \leq f_4^\gamma \leq 1.0$	$-3.3 \leq f_5^\gamma \leq 3.2$

In order to calculate the impact of anomalous couplings on the measured distributions in the process $e^+e^- \to f\bar{f}f'\bar{f}'$, the EXCALIBUR generator is extended to have all matrix elements of conversion diagrams with two Z bosons supplemented by an additional term containing anomalous couplings. Using the experimental distributions a binned maximum likelihood fit is performed for each of the anomalous couplings f_i^V fixing the others to zero. The function maximized is:

$$\log L = \sum_{\text{bins}} (N^i_{data} \cdot log N^i_{MC} - N^i_{MC}) \tag{2}$$

where $N^i_{MC} = N^i_{ZZ}(f^{Z,\gamma}_{4,5}) + N^i_{bkgd}$ is the computed sum of background and signal contribution taking into account the anomalous coupling. The results for all couplings are consistent with the Standard Model values of zero and 95% confidence level limits on the parameters f_i^V are set as are swown in Tab. 3

The 189 GeV results are preliminary.

6 Conclusions

Using the data collected from L3 detector at center-of-mass energy of 183 GeV and 189 GeV the production of ZZ pair has been investigated.
The cross section measured is in agreement with the predicted Standard Model value.
No evidence for existence of anomalous ZZZ and ZZγ is found.

7 Acknowledgements

I would like to tank Dr. Eusebio Sanchez and Prof. Joachim Mnich for critical reading of manupscript.

References

1. L3 Collab., M. Acciarri *et al.*, Phys. Lett. **B 450** (1999) 281.

2. L3 Collaboration, "Preliminary Results on Neutral Gauge Boson Production in e^+e^- interactions at $\sqrt{s} = 189$ GeV", L3 Note 2366, March 5, 1999.

3. F.A. Berends, R. Kleiss and R. Pittau, Nucl. Phys. **B 424** (1994) 308; Nucl. Phys. **B 426** (1994) 344; Nucl. Phys. (Proc. Suppl.) **B 37** (1994) 163; Phys. Lett. **B 335** (1994) 490; R. Kleiss and Pittau, Comp. Phys. Comm. **83** (1994) 14.

4. K. Hagiwara *et al.*, Nucl. Phys. **B 282** (1987) 253.